



# Developing a membrane-proximal CD33-targeting CAR T cell

Ruby Freeman,<sup>1</sup> Sanam Shahid ,<sup>1</sup> Abdul G Khan,<sup>1</sup> Serena C Mathew,<sup>1</sup> Sydney Souness,<sup>1</sup> Erin R Burns,<sup>1</sup> Jasmine S Um,<sup>1</sup> Kento Tanaka,<sup>1</sup> Winson Cai,<sup>1</sup> Sarah Yoo,<sup>1</sup> Andrew Dunbar,<sup>1</sup> Young Park,<sup>1</sup> Devin McAvoy,<sup>1</sup> Kinga K Hosszu,<sup>1</sup> Ross L Levine,<sup>1</sup> Jaap Jan Boelens,<sup>1</sup> Ivo C Lorenz,<sup>1</sup> Renier J Brentjens,<sup>2</sup> Anthony F Daniyan <sup>1</sup>

**To cite:** Freeman R, Shahid S, Khan AG, *et al.* Developing a membrane-proximal CD33-targeting CAR T cell. *Journal for ImmunoTherapy of Cancer* 2024;**12**:e009013. doi:10.1136/jitc-2024-009013

► Additional supplemental material is published online only. To view, please visit the journal online (<https://doi.org/10.1136/jitc-2024-009013>).

RF and SS are joint first authors.

RJB and AFD are joint senior authors.

Accepted 11 April 2024



© Author(s) (or their employer(s)) 2024. Re-use permitted under CC BY-NC. No commercial re-use. See rights and permissions. Published by BMJ.

<sup>1</sup>Memorial Sloan Kettering Cancer Center, New York, New York, USA

<sup>2</sup>Roswell Park Comprehensive Cancer Center, Buffalo, New York, USA

## Correspondence to

Renier J Brentjens;  
[renier.brentjens@roswellpark.org](mailto:renier.brentjens@roswellpark.org)

## ABSTRACT

**Background** CD33 is a tractable target in acute myeloid leukemia (AML) for chimeric antigen receptor (CAR) T cell therapy, but clinical success is lacking.

**Methods** We developed 3P14HLh28Z, a novel CD33-directed CD28/CD3Z-based CAR T cell derived from a high-affinity binder obtained through membrane-proximal fragment immunization in humanized mice.

**Results** We found that immunization exclusively with the membrane-proximal domain of CD33 is necessary for identification of membrane-proximal binders in humanized mice. Compared with clinically validated lintuzumab-based CAR T cells targeting distal CD33 epitopes, 3P14HLh28Z showed enhanced *in vitro* functionality as well as superior tumor control and increased overall survival in both low antigen density and clinically relevant patient-derived xenograft models. Increased activation and enhanced polyfunctionality led to enhanced efficacy.

**Conclusions** Showing for the first time that a membrane-proximal CAR is superior to a membrane-distal one in the setting of CD33 targeting, our results demonstrate the rationale for targeting membrane-proximal epitopes with high-affinity binders. We also demonstrate the importance of optimizing CAR T cells for functionality in settings of both low antigen density and clinically relevant patient-derived models.

## INTRODUCTION

Acute myeloid leukemia (AML) is the most common and lethal form of acute leukemia in adults. Despite the addition of novel agents to the intensive chemotherapeutic backbone and consolidative allogeneic stem cell transplantation therapy, long-term clinical outcomes are relatively poor, particularly after disease relapse.<sup>1</sup> Hence, novel therapeutics are needed to improve these dismal outcomes.

Chimeric antigen receptor (CAR) T cells are the most potent form of adoptive immunotherapy and have revolutionized the treatment of B-cell acute and chronic malignancies. However, CAR T cells do not lead to durable disease control in a majority of patients.<sup>2 3</sup> CAR T cell rejection has been associated with

## WHAT IS ALREADY KNOWN ON THIS TOPIC

⇒ CD33-directed chimeric antigen receptor (CAR) T cell preclinical evaluation to-date has determined that the combination of a targeting motif derived from lintuzumab (HuM195, SGN-33; an antibody that targets the distal CD33-IgV domain) linked to CD28/CD3Z provides the best-in-class CAR construct, which has since moved into the clinic; however, clinical efficacy has been limited.

## WHAT THIS STUDY ADDS

⇒ We developed a fully human-derived CAR T cell that targets the membrane-proximal IgC domain of CD33 (CD33-IgC) and improves preclinical CAR T cell efficacy compared with clinically validated lintuzumab-based CAR T cells targeting distal CD33 epitopes.

## HOW THIS STUDY MIGHT AFFECT RESEARCH, PRACTICE OR POLICY

⇒ Our data support targeting CD33-IgC to markedly enhance the efficacy of CAR T cells for acute myeloid leukemia treatment.  
⇒ Our promising preclinical data warrant rapid translation of membrane-proximal CD33-targeting CAR T cells to the clinic.

non-human-derived sequences of targeting motifs, impaired effector cell proliferation, reduced polyfunctionality, and inability to eliminate low-antigen-density tumor subpopulations, leading to suboptimal outcomes.<sup>4-8</sup> In a recent phase I trial of autologous CD33-directed 4-1BB/CD3Z CAR T cells for the treatment of relapsed/refractory (R/R) AML, low T cell numbers at apheresis and high, progressive tumor burden were major challenges to clinical deployment of the manufactured product.<sup>9</sup> Hence, for CAR T cell therapies to be successful in AML, CAR design must address these major roadblocks.

Unlike with CD19 in B-cell malignancies, there is no single tumor-associated antigen defining AML cells. Many AML-associated antigens are present on non-malignant

myeloid cell populations, making myelosuppression obligatory.<sup>10</sup> CD33, a sialoadhesin consisting of membrane-distal immunoglobulin variable (IgV) and membrane-proximal immunoglobulin constant (IgC) domains, has emerged as a tractable target given its near ubiquitous expression on AML cells. Importantly, CD33 is also present on progenitor/mature myeloid and hematopoietic stem cells (HSCs) but not required for human myeloid development and function,<sup>11,12</sup> allowing for strategies that ablate both the entire CD33-positive malignant and normal hematopoietic compartment, followed by hematopoietic rescue using engineered CD33-negative HSCs.

Targeting CD33 is further complicated by the rs12459419 C>T single nucleotide polymorphism (SNP), which is associated with decreased CD33 surface expression.<sup>13,14</sup> Although the clinical relevance of this SNP is debatable, >50% of patients possess the CT or TT genotype, leading to reduced or absent surface expression of CD33.<sup>13–16</sup> Hence, CD33 CAR T cells must recognize low-antigen-density AML. Preclinical studies have reported CD33 CAR T cells showing potent activity, with some employing strategies to limit the duration of this activity to allow for rescue with allogeneic stem cell transplantation.<sup>17,18</sup> However, whether these CAR T cells can function in the presence of high-antigen-density and low-antigen-density targets, as well as in the context of clinically relevant patient-derived AML models, has not been well described.

A recent study describing a rigorous preclinical approach to optimize CD33-directed CAR T cells determined that the combination of a targeting motif derived from lintuzumab (HuM195, SGN-33; an antibody that targets the distal CD33 IgV domain) linked to CD28/CD3Z provided the best-in-class CAR construct, which has moved to the clinic (NCT03971799).<sup>19,20</sup> Here, we intended to improve on the lintuzumab-CD28/CD3Z (H195HLh28Z) platform by developing a fully human-derived CAR T cell that targets the membrane-proximal IgC domain of CD33 (CD33-IgC), as such proximal epitope targeting has been shown to improve CAR T cell efficacy.<sup>21–24</sup>

We demonstrated that raising antibodies to CD33-IgC requires immunization of this fragment alone, as full-length CD33 immunization always led to IgV-specific binders in our humanized rodent system. High-affinity CD33-IgC-targeting CAR T cells had greater proliferative capabilities and increased polyfunctionality *in vitro* compared with H195HLh28Z, leading to improved survival and tumor control in both low antigen density and clinically relevant patient-derived xenograft (PDX) models. Interestingly, membrane-proximal CD33-IgC-targeting CAR T cells demonstrated superior functionality compared with membrane-distal-targeting H195HLh28Z. Collectively, our data support targeting CD33-IgC to markedly enhance the efficacy of CAR T cells for AML treatment.

## METHODS

### Cell lines

Two hundred ninety-three Glv9-packaging cells (courtesy of the Sadelain lab, MSK, New York, New York, USA) were maintained in DMEM (Dulbecco's Modified Eagle Medium) with high-glucose supplemented with 10% heat-inactivated FBS (fetal bovine serum) non-essential amino acids (Atlanta Biological Flowery Branch), 2 mM L-glutamine (Invitrogen), and 1% penicillin/streptomycin (Invitrogen). The U937 human acute leukemia line (courtesy of the Levine lab, MSK), the OCiAML3 human acute myeloid leukemia line (courtesy of the Bachovin lab, MSK), and the MOLM14 human acute myeloid leukemia line (courtesy of the Kung lab, MSK) were modified to express green fluorescent protein-firefly luciferase (gfpLuc) to detect tumor *in vitro* and *in vivo* by luminescence. All tumor cell lines were maintained in RPMI-1640 medium supplemented with 10% heat-inactivated FBS non-essential amino acids (Atlanta Biological Flowery Branch), 10 mM HEPES (hydroxyethyl piperazineethanesulfonic acid, Invitrogen), 2 mM L-glutamine (Invitrogen), 1% penicillin/streptomycin (Invitrogen), and 11 mM glucose (Invitrogen). Cell lines were routinely tested for potential mycoplasma contamination.

### Selection of single-chain variable fragment (scFv)

Antibody generation and characterization studies were carried out by the Tri-Institutional Therapeutics Discovery Institute (TriI-TDI) using AlivaMab transgenic mice (Ablexis) with the extracellular domain of CD33 recombinant proteins either sourced commercially or produced in-house. Recombinant human CD33 protein was sourced commercially from R&D Systems and Acro Biosystems. Mouse and cynomolgus monkey CD33 proteins were purchased from Sino Biological. In addition, human CD33-IgC domain (residue 140–259) with a terminal mouse IgG1 Fc or 6xHis tag was produced in-house. Immunizations and screenings were carried out at LakePharma (Belmont, California, USA). Multiple cohorts of AlivaMab mice were immunized with recombinant proteins, with one cohort receiving CD33-IgC. Serum was collected on days 17, 24, 28, and 31, and the immune response was analyzed by ELISA using recombinant human full-length CD33-6xHis and CD33 IgC2-6xHis proteins. Hybridomas were generated by electrofusion, and the supernatants were screened by ELISA on recombinant proteins as well as by flow cytometry on 3T3 cells overexpressing either full-length CD33 or CD33-IgC alone and AML cell lines with endogenous CD33 expression. Subcloning was performed by limited dilution, and sequencing of the top 10 lead candidates was carried out using standard IgG primers recommended by Ablexis.

### Binding selectivity and affinity

Lead and reference antibodies were produced recombinantly with a human IgG1 constant region. Selectivity was tested using His tag recombinant human full-length CD33 or CD33-IgC, mouse full-length CD33, and cynomolgus

full-length CD33 proteins. Recombinant proteins at 5 µg/mL were captured by pre-blocked Ni-NTA plates. Candidate antibodies were added at 10 µg/mL in triplicate and detected using horseradish peroxidase-conjugated anti-human Fc antibody. To assess the binding to cell-surface-bound CD33, 3T3 cells overexpressing CD33, as well as the U937 AML cell line, were used. U937 CD33-knockout (CD33KO) or 3T3 wild-type cells were included as negative controls. U937 CD33+ and CD33KO cells were blocked with human IgG Fc for 20 min on ice. The recombinant antibodies were then serially diluted starting at 100 µg/mL concentration and added for 30 min on ice. Alexa Fluor 647-conjugated goat anti-human F(ab')<sub>2</sub> was added to cells for 30 min on ice, washed and analyzed by flow cytometry, and normalized to secondary-only staining (mean fluorescence intensity (MFI) ratio). EC<sub>50</sub> values were determined by non-linear regression. The binding affinity and epitope binning to human CD33 protein was measured by biolayer interferometry (BLI) using an Octet Red96e. All experiments were carried out using kinetic buffer (Phosphate-buffered saline (PBS) pH 7.4, 0.01% BSA, 0.002% Tween-20). For affinity measurements, the antibodies were captured by an anti-huFc biosensor, and a 7-point, twofold dilution series of huCD33-His was used as analyte. The data were processed by double reference subtraction, and response curves were globally fit to a 1:1 Langmuir binding model.

### Generation of retroviral constructs

Constructs were cloned into the SFG gammaretroviral vector with human signaling domains. Retroviral producer cell lines were generated by using CaPO4 (Promega) according to the manufacturer's instructions to transiently transfect gpg29 fibroblasts (H29) with retroviral constructs encoding the CAR. Supernatant from the H29 cells was used to transduce 293Glv9 to produce stable retroviral producer cell lines. Final constructs produced were 3P14HLh28Z, 4B2AHLh28Z, and H195h28Z, as well as H195DEL, which served as a non-signaling control and was generated by deletion of the cytosolic domains encoding CD28 and CD3Z.

### T cell isolation and retroviral transduction

Briefly, peripheral blood mononuclear cells (PBMCs) were isolated from healthy donor peripheral blood or leukopaks (New York Blood Center). Following red blood cell lysis with ACK (ammonium-chloride-potassium) Lysing Buffer (Lonza), human T cells were isolated from PBMCs (StemCell Technologies) and subsequently activated with 100 IU/mL of IL-2 and Dynabeads Human T-Activator CD3/CD28 at a bead:cell ratio of 1:5 (Thermo Fisher Scientific). Forty-eight hours after initial expansion, T cells were spinoculated with viral supernatant collected from 293Glv9 packaging cells on RetroNectin-coated plates on 2 consecutive days (Takara Clontech). All experiments were normalized for CAR+ viable cells.

### Flow cytometry

Flow cytometric analyses were performed using 10-color Gallios B43618 (Beckman Coulter, Indianapolis, Indiana, USA) and 14-color Attune NxT (Thermo Fisher Scientific) instruments. Data were analyzed using FlowJo (Tree Star) V.10.8.0. Flow cytometry was used to determine transduction efficiency of transduced cells following staining with phycoerythrin (PE)-conjugated cetuximab antibody and Myc-tag (9B11, Alexa Fluor 647, Cell Signaling). DAPI (0.5 mg/mL, Sigma Aldrich) or 7-amino-actinomycin D (0.05 mg/mL, BioLegend) and PO-PRO-1 Iodine (Invitrogen) staining were used to exclude dead cells in all experiments. Antibodies are listed in online supplemental table 1. All antibodies were purchased from BioLegend, BD Biosciences, Invitrogen or eBioscience.

### Cytotoxicity assays

The cytolytic capacity of CAR-modified human T cells was assessed through a luciferase-killing assay. CAR T cells were co-cultured with  $1 \times 10^4$  target cells, U937-CD33<sup>high</sup> or OCiAML3-CD33<sup>low</sup> tumor cells, at various effector-to-target ratios in quadruplicate in white-walled 96-well plates (Thermo Scientific) in a total volume of 200 µL of cell media. Target cells were plated with non-signaling control CAR T cells (H195DEL) at the same cell densities to determine maximal luciferase expression as a reference (max signal). Twenty-four hours or 96 hours later, 15 µg D-Luciferin (Gold Biotechnology) dissolved in 50 µL PBS was added to each well. Emitted luminescence of each sample (sample signal) was detected in a Spark plate reader (Tecan) and measured using SparkControl software (Tecan). Percent lysis was determined as:  $100 - [(sample\ signal/average\ max\ signal) \times 100]$ .

### Proliferation assays

CAR T cells were co-cultured with U937-CD33<sup>high</sup> tumor cells at 1:2.5 or 1:10 CAR T:tumor cell ratio. After 7 days, flow cytometry was used to detect tumor and T cells after staining with fluorescently labeled cetuximab. CAR T cells were re-stimulated with fresh tumor cells at the same 1:2.5 or 1:10 CAR T:tumor cell ratio. The procedure above was repeated weekly for 21 days after initial stimulation.

### In vitro cytokine secretion analysis

To measure in vitro T cell cytokine production, CAR T cells were co-cultured in a 1:1 ratio for 24 hours with antigen-positive tumor cells or antigen-negative tumor cells in a 96-well round-bottom plate. Twenty-four hours later, the supernatant fluid was collected and analyzed for cytokines on a Luminex IS100 instrument. Luminex FlexMap3D system, Luminex xPONENT 4.2, and 12-plex Human panel (Millipore) were used to detect cytokines.

### Intracellular flow cytometry for polyfunctionality

To measure intracellular T cell cytokine and granzyme B production, CAR T cells were co-cultured at a 1:5 with U937-CD33<sup>high</sup> tumor cells. Approximately 16 hours later, a 500X Protein Transport Inhibitor cocktail was added to the cell culture (eBiosciences), and 6 hours later, cells

were collected, stained with Fixable Yellow Dead stain (ThermoFisher Scientific), and fixed and permeabilized with BD Cytofix/Cytoperm Fixation and Permeabilization Solution (BD Biosciences) as per the manufacturer's suggested protocol. Cells were counted and stained with the following human antibodies: cetuximab-conjugated in-house with PE, anti-CD4 (RPA-T4), anti-CD8 (SK1), anti-IL-2 (MQ1-17H12), anti-TNF-alpha (MAb11), anti-IFN-gamma (4S.B3), and anti-granzyme B (QA16A02).

### Multiparametric flow cytometric analysis

Cells were washed with PBS, resuspended in PBS at a concentration of  $3.0 \times 10^6$ /mL, and incubated with Human TruStain FcX Fc receptor blocking solution (BioLegend) and Live/DEAD Fixable Blue Dead Cell Stain (Invitrogen) according to the manufacturers' specifications for 20 min at room temperature, protected from light. The cells were then washed once in Flow Wash Buffer (FWB; RPMI 1640, no phenol red+4% FBS+0.01% sodium-azide). Cells were incubated with the antibody mix for 20 min at room temperature in the dark in 100  $\mu$ L staining volume in the presence of Super Bright Staining Buffer (eBiosciences), washed twice in FWB, resuspended in 0.5% paraformaldehyde/PBS, and immediately acquired using a Cytex Aurora 5L flow cytometer (Cytex). Antibodies are listed in online supplemental table 1.

### Animal models

All experiments were performed in accordance with the Memorial Sloan Kettering Cancer Center (MSK) Institutional Animal Care and Use Committee (IACUC) approved guidelines (MSK #00-05-065). For xenogeneic studies, NOD-*Prkdc<sup>em26Cd52</sup>Il2rg<sup>em26CD22</sup>/NjuCrl*, Coisogenic Immunodeficient (NCG) mice were purchased from Charles River and subsequently bred and housed under specific-pathogen-free conditions in the animal facility of MSK. For all experiments, mice 6–12 weeks old were used. Male and female mice were used with equal outcomes. Animal users were not blinded.

### In vivo experiments

For CD33-high tumor studies,  $5 \times 10^4$  U937 or  $1 \times 10^6$  MOLM14 AML cells expressing gfpLuc were inoculated on day 0. For CD33-low tumor studies,  $5 \times 10^5$  OCiAML3 AML cells expressing gfpLuc were inoculated on day 0. In both models, mice were treated with varying doses of CAR T cells via tail vein 3 days after tumor inoculation. All tumor cells produced very even tumor burdens and no mice were excluded prior to treatment. Day 0 bioluminescence was assigned to be  $1 \times 10^7$ . Tumor burden was measured weekly using bioluminescence imaging using the Xenogen IVIS Imaging system (Xenogen) with Living Image software (Xenogen).

For the AML60B pPDX model, viably cryopreserved primary AML specimens were obtained via an Institutional Review Board-approved research protocol (MSKCC IRB 17-268). NCG mice were inoculated with  $1 \times 10^6$  cells on day 0. On day 10, mice were randomized

into different treatment cohorts and subsequently treated with  $1 \times 10^6$  CAR T cells via tail vein. On day 28, bone marrow aspirations were performed, and tumor cells were quantified by flow cytometry.

### Statistical analysis

All statistical analyses were performed using GraphPad Prism software (GraphPad). Data points represent biological replicates and are shown as the mean $\pm$ SEM as indicated in the figure legends. Statistical significance was determined by paired t-test, one-way analysis of variance (ANOVA), or two-way ANOVA as indicated in the figure legends. The log-rank (Mantel-Cox) test was used to determine statistical significance for overall survival in mouse survival experiments. Significance was indicated with \* $p < 0.05$ , \*\* $p < 0.01$ , \*\*\* $p < 0.001$ , and \*\*\*\* $p < 0.0001$ .

## RESULTS

### CD33-IgC immunization is necessary for discovery of site-specific binders

To generate CD33-IgC-specific antibodies, we immunized Ablexis' AlivaMab mice with either full-length CD33 or CD33-IgC recombinant proteins, as it was unknown whether the distal IgV domain would be critical to retain an IgC conformation necessary for immunological recognition. Hybridomas were generated and 53 hits were identified by ELISA using recombinant human CD33. On-cell binding was assessed by flow cytometry on 3T3 cells (mouse fibroblast cell line) expressing either full-length CD33 or CD33-IgC, as well as U937 (AML cell line) with endogenous CD33 expression (figure 1A). The specificity of binders was tested by screening U937, a cell line that naturally expresses CD33 in which CD33 was knocked-out using CRISPR/Cas9, and 3T3, a murine cell line that does not express CD33 in which CD33 was knocked-in using CRISPR/Cas9 (online supplemental figure 1A,B). Interestingly, all CD33-IgC domain-specific antibodies exhibiting consistent binding to various cell lines were derived from the CD33-IgC immunized cohort only. From this group, three hybridomas were selected and sequenced, resulting in the identification of two unique clones, 3P14 and 4B2A.

Next, we confirmed the binding specificity and affinity of 3P14, 4B2A, and a reference CD33-IgV-specific monoclonal antibody (mAb), lintuzumab (H195). Antibodies were recombinantly expressed as human IgG1 subclass. All mAbs bound full-length human CD33, but not cynomolgus or mouse orthologs, and as expected only 3P14 and 4B2A bound human CD33-IgC (online supplemental figure 1C). Using BLI, all mAbs had similar binding affinities for recombinant full-length CD33, with similar dissociation constants ( $K_D$ ) and on-rates, but with a log lower off-rate for H195 compared with 3P14 and 4B2A (online supplemental figure 1D). Given that mAbs could have varying affinities for soluble versus cell-bound antigen, we measured their binding to cell-surface CD33, using 3T3 cells overexpressing the antigen (3T3-CD33) as well as a

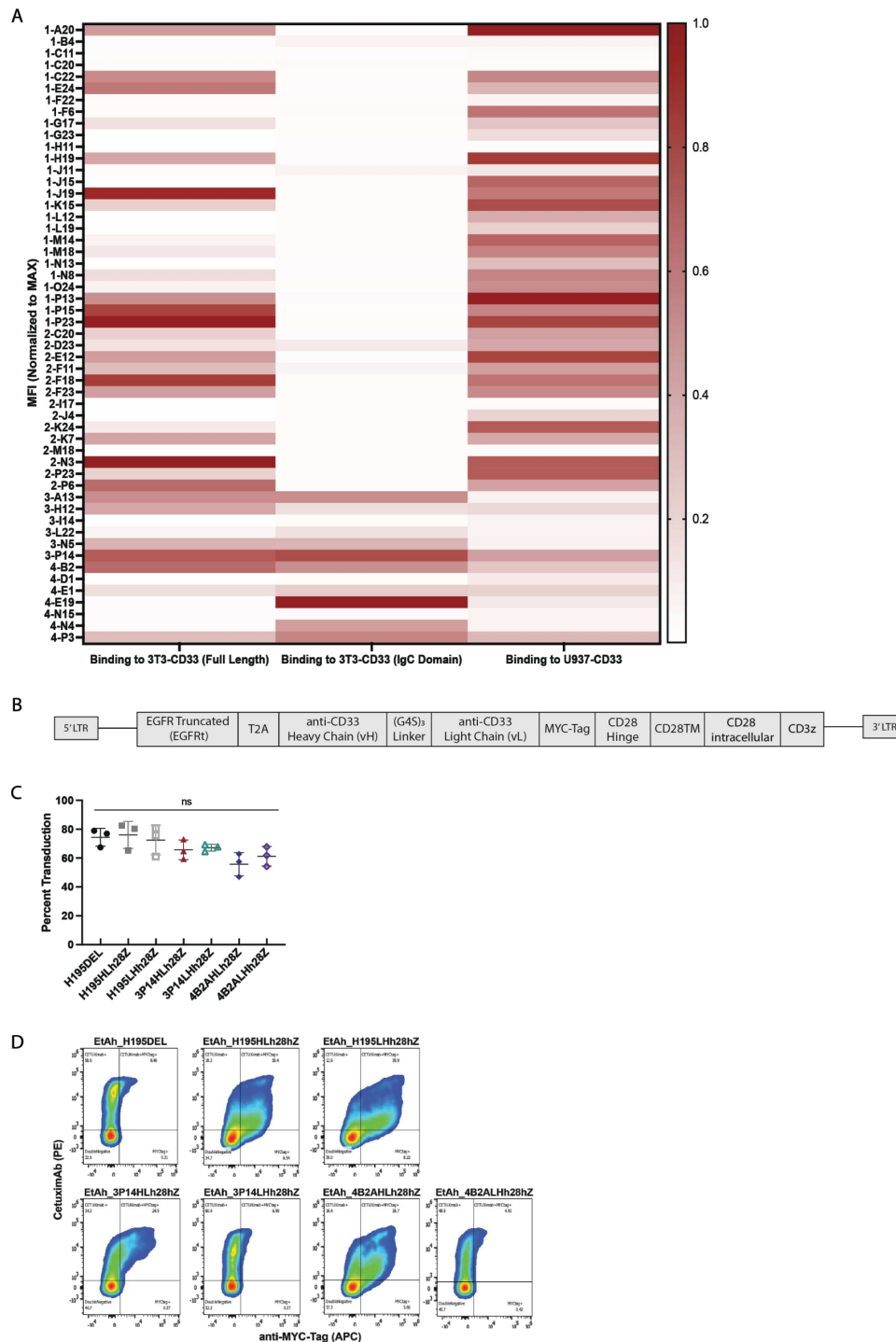


**Figure 1** Identification of a membrane-proximal CD33 antibody. (A) Heatmap showing relative binding of selected antibodies to human full-length CD33, CD33-IgC, and U937 CD33-expressing tumor lines. (B) Schematic representation of retroviral vector encoding 5' and 3' long terminal repeats sequence (LTR), truncated EGFR, linked with a T2A element to a fully human CD33-targeted single-chain variable fragment, human CD28 hinge, transmembrane, and intracellular domains (CD28), and human zeta chain signaling domain (z chain). A Myc-tag is included for detection of the chimeric antigen receptor (CAR). (C) Summary data of retroviral transduction efficiency of CAR constructs as determined by flow cytometry using cetuximab. P values determined by repeated measures one-way analysis of variance. Data are a mean $\pm$ SEM of three biological replicates conducted in three independent experiments; ns, non-significant. (D) Representative flow cytometry plot demonstrating CAR expression following human T cell transduction, detected with fluorescently labeled Cetuximab and Myc-Tag-specific antibodies. MFI, mean fluorescence intensity.

relevant AML tumor cell line, U937, which has endogenous expression of CD33. The hierarchy of affinity, from highest to lowest, was H195>3P14>4B2A, with the most pronounced differences noted for U937 cells (online supplemental figure 1D,E).

Next, we used epitope binning with immobilized CD33 to determine if 3P14 and 4B2A bound to similar epitopes, and if their differing affinities influenced binding of one antibody over another (online supplemental methods). We observed that, when 3P14 was the saturating mAb, 4B2A was unable to demonstrate binding (0%), and when 4B2A was the saturating mAb, 3P14 was able to bind (68%); no binding competition was observed between H195 and either 3P14 or 4B2A (online supplemental figure 1F), indicating that while 3P14 and 4B2A may have overlapping epitopes, both differed from membrane-distal H195.

Next, we generated scFvs of H195, 3P14, and 4B2A in both the VH-VL (HL) and VL-VH (LH) orientations and cloned these into a bicistronic vector containing a truncated epidermal growth factor receptor tag (EGFRt) and a Myc-tag in line with human CD28/CD3Z (h28Z) signaling motifs (figure 1B). For consistency, transduction was assessed by EGFR positivity, which was similar across all constructs (figure 1C). We stained for the Myc-tag and found that the HL formats more reliably demonstrated cell-surface CAR expression (figure 1D).

These data show that CD33-IgC immunization is critical for raising binders to this domain in humanized rodent systems, and that 3P14 binds with a higher affinity to CD33-IgC and likely recognizes a similar epitope to 4B2A, given the capacity of the former to displace the latter during epitope binning. These data also suggest that, because the HL scFv orientation more consistently demonstrates CAR surface expression of our candidate binders, it is the preferred format for preclinical testing.

### CAR T cells targeting CD33-IgC demonstrate enhanced functionality in vitro

Low surface antigen density and excessive tumor burden are major mechanisms of resistance and treatment failure, leading to impaired tumor control and reduced effector expansion of CAR T cells for specific CAR T products and specific diseases that have been evaluated to-date.<sup>4 5 25</sup> The CT or TT genotypes of the rs12459419 C>T SNP are present in ~50% of patients with AML, resulting in low CD33 surface expression on malignant cells. Using flow cytometry, we determined CD33 expression levels on three cell lines with s12459419 C>T SNP genotype reported: MOLM14 (CC), U937 (CT), and OCiAML3 (TT).<sup>19 21</sup> MOLM14 and U937 cell lines expressed equivalent CD33 expression, so we selected these to characterize high-expressing CD33 models, whereas OCiAML3 cell line demonstrated lower CD33 expression in comparison (figure 2A,B, online supplemental table 2). Target cell lines were transduced with a gfpLuc to generate U937-CD33<sup>high</sup>gfpLuc<sup>+</sup> (U937-CD33<sup>high</sup>),

MOLM14-CD33<sup>high</sup>gfpLuc<sup>+</sup> (MOLM14-CD33<sup>high</sup>), and OCiAML3-CD33<sup>low</sup>gfpLuc<sup>+</sup> (OCiAML3-CD33<sup>low</sup>) for in vitro and in vivo tracking (data not shown).

Next, we determined the capacity of CD33-IgC-specific CAR T cells to kill tumor cells with high and low CD33 antigen density. In 24-hour killing assays at varying effector-to-target (E:T) ratios (1:1 to 1:128), 3P14HLh28Z and 4B2AHLh28Z showed increased dose-dependent killing of U937-CD33<sup>high</sup> and MOLM14-CD33<sup>high</sup> at low E:T ratios compared with H195HLh28Z, but 3P14HLh28Z demonstrated enhanced cytotoxicity against OCiAML3-CD33<sup>low</sup> cells at slightly higher ratios (figure 2C). In 96-hour long-term killing assays using the same E:T ratios (1:1 to 1:128), 3P14HLh28Z and 4B2AHLh28Z showed superior tumor control of all tumor cell lines compared with H195HLh28Z especially at higher E:T ratios (figure 2D). Percent CAR positivity is shown in online supplemental figure 2.

To validate CD33-IgC specificity of 3P14HLh28Z and 4B2AHLh28Z, we transduced U937-CD33<sup>KO</sup> cells with a retroviral vector encoding a modified FLAG-tagged CD33-IgC, and surface expression was confirmed by flow cytometry (online supplemental figure 3A and online supplemental table 2). Compared with H195HLh28Z, both 3P14HLh28Z and 4B2AHLh28Z lysed CD33-IgC-expressing target cells in a dose-dependent manner (online supplemental figure 3B). Importantly, no CAR T cell lysed the negative control U937-CD33<sup>KO</sup> (online supplemental figure 3C). Given the reported expression of low levels of CD33 on HSCs, we utilized a colony-forming unit (CFU) assay to determine if 3P14HLh28Z and 4B2AHLh28Z could detect and eliminate these cells (online supplemental methods). We observed complete ablation of colonies with only 3P14HLh28Z and high-dose gemtuzumab ozogamicin (GO), which served as a positive control, and incomplete ablation of colonies with either 4B2AHLh28Z or H195HLh28Z CAR T cells (online supplemental figure 3D).

Given the relevance of CAR T cell expansion to clinical efficacy, we tested the proliferative capacity of 3P14HLh28Z and 4B2AHLh28Z in the context of recursive stimulation with high CD33 antigen density targets. 3P14HLh28Z had increased expansion and persistence compared with other CAR T cells when co-cultured with U937-CD33<sup>high</sup> at two different E:T ratios (figure 2E).

In summary, our data show that high-affinity CD33-IgC-specific 3P14HLh28Z is superior functionally to low-affinity CD33-IgC-specific 4B2AHLh28Z and high-affinity CD33-IgV-specific H195HLh28Z in the setting of high-tumor burden, as assessed by recursive stimulation or low-antigen-density encounters. Furthermore, low-affinity, membrane-proximal 4B2HLh28Z exhibited superior CAR T activity compared with high-affinity, membrane-distal H195HLh28Z, underscoring the importance of antigen target proximity in the context of CD33 CAR T cells.

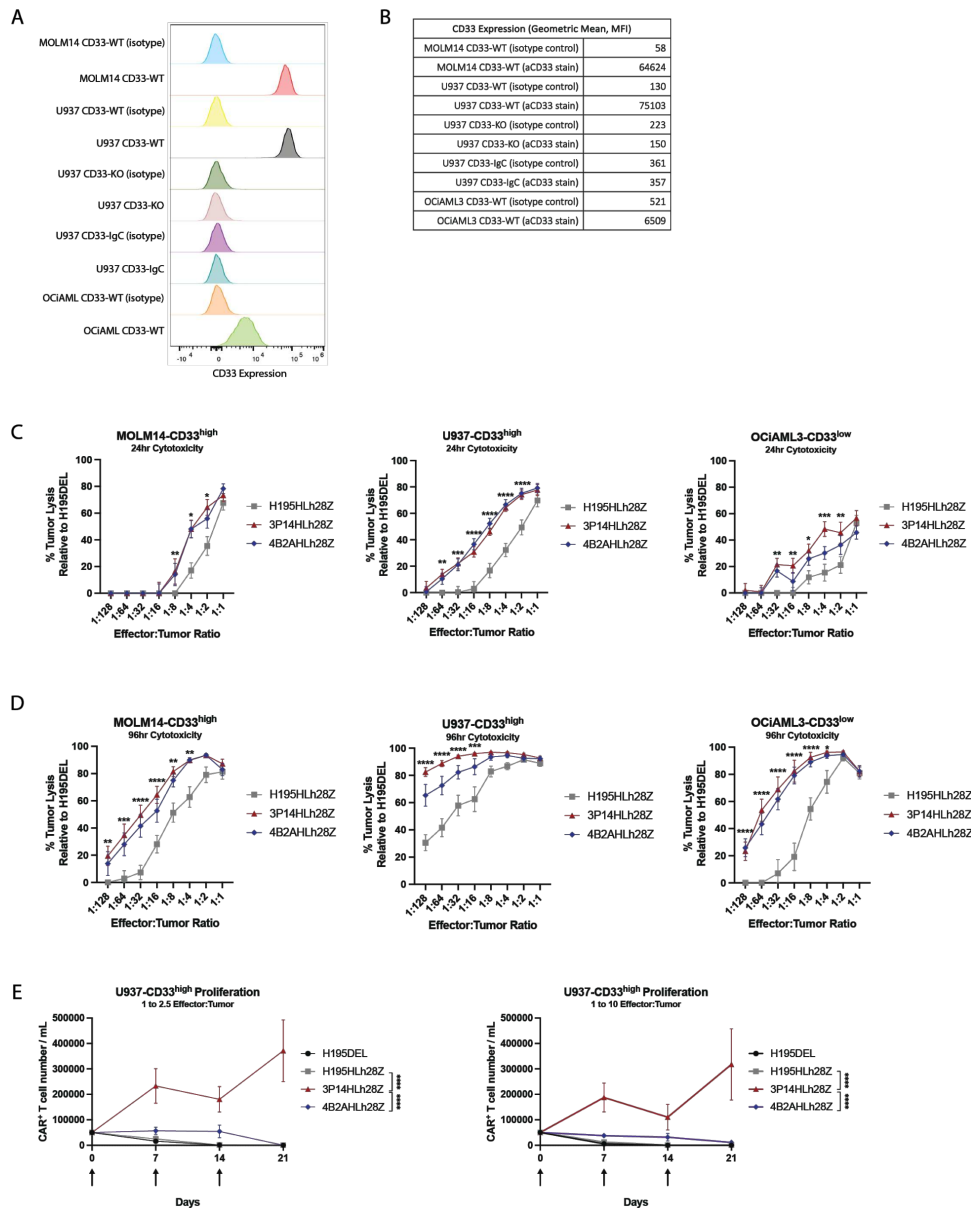


**Figure 2** Membrane-proximal targeting chimeric antigen receptor (CAR) T cells demonstrate enhanced functionality and proliferative capacity in vitro. (A) Flow cytometry histograms of CD33 expression on acute myeloid leukemia (AML) cells detected with isotype control or fluorescently labeled CD33-specific antibody. (B) Quantitative geometric mean fluorescence intensity (MFI) of CD33 expression on AML cells detected with either isotype control or fluorescently labeled CD33-specific antibody. (C) 24-hour D-luciferin assay demonstrating lysis of CD33-expressing tumor cells ( $n=4$  biological replicates; \*\*\*\* $p<0.0001$ ; \*\*\* $p<0.001$ ; \*\* $p<0.01$ ; \* $p<0.05$  by two-way analysis of variance (ANOVA)). Data are a mean $\pm$ SEM of four biological replicates. (D) 96-hour D-luciferin assay demonstrating lysis of CD33 expressing tumor cells ( $n=4$  biological replicates; \*\*\*\* $p<0.0001$ ; \*\*\* $p<0.001$ ; \*\* $p<0.01$ ; \* $p<0.05$  by two-way ANOVA). Data are a mean $\pm$ SEM of four biological replicates. (E) Quantification of flow cytometric analysis demonstrating enhanced proliferation by membrane-proximal CD33 targeting CAR T cell in the presence of U937-CD33<sup>high</sup> tumor cells at E:T ratios of 1:2.5 (left) or 1:10 (right) ( $n=3$  biological replicates; \*\*\*\* $p<0.0001$  by two-way ANOVA at day 21). Arrows indicate when additional target cells were added. Data are a mean $\pm$ SEM of three biological replicates.

### CAR T cells targeting CD33-IgC with high affinity are polyfunctional

To identify the mechanism of enhanced functionality of 3P14HLh28Z, we assessed the 24-hour in vitro cytokine production by co-culturing CAR T cells with U937-CD33<sup>high</sup> or OCIAML3-CD33<sup>low</sup>. 3P14HLh28Z secreted elevated levels of Tc1/Th1 cytokines in a target-specific manner as compared with both 4B2AHLh28Z and

H195HLh28Z (figure 3A and online supplemental figure 4). Given the higher cumulative cytokine production by 3P14HLh28Z, we determined the role of polyfunctionality, which has been associated with enhanced clinical responses.<sup>6</sup> After 24 hours of CAR T cell and U937-CD33<sup>high</sup> co-culture, at an E:T ratio of 1:5, intracellular flow cytometry showed increased levels of IFN- $\gamma$ , IL-2, Granzyme B, and TNF- $\alpha$  with 3P14HLh28Z versus

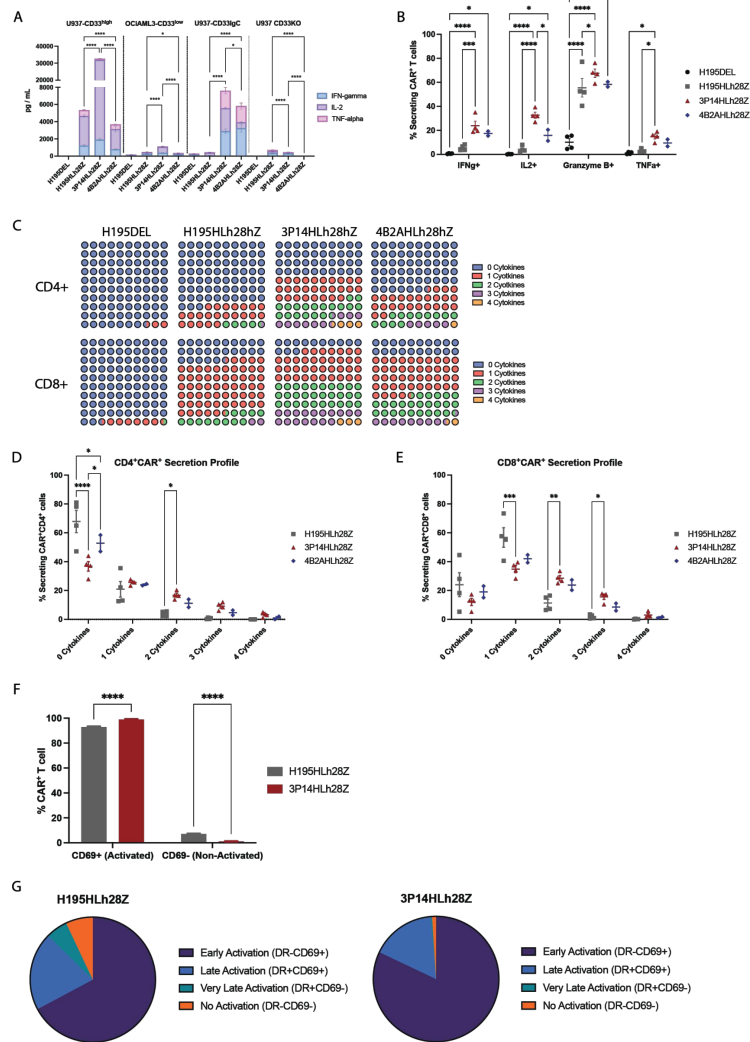


**Figure 3** Membrane-proximal targeting chimeric antigen receptor (CAR) T cells are characterized by a unique activation profile in vitro. (A) 24-hour cytokine secretion profile of Tc1/Th1 cytokines when co-cultured with U937-CD33<sup>high</sup>, OCiAML3-CD33<sup>low</sup>, U937-CD33<sup>lgC</sup>, and U937-CD33<sup>KO</sup> tumor as detected by human 12-plex Luminex panel (n=3; \*\*\*\*p<0.0001; \*p<0.05 by Dunnett's multiple comparison tests against H195DEL control). Data are a mean±SEM of three biological replicates conducted in three independent experiments. (B) Quantification of flow cytometric analysis showing CAR T cell intracellular production of Tc1/Th1 activation cytokines when cultured with U937-CD33<sup>high</sup> tumor (n=4; \*\*\*\*p<0.0001; \*\*p<0.01; \*p<0.05 by two-way analysis of variance (ANOVA); ns, non-significant). Data are a mean±SEM of four biological replicates conducted in three independent experiments. (C) Qualitative representation of CD4<sup>+</sup>CAR<sup>+</sup> and CD8<sup>+</sup>CAR<sup>+</sup> Tc1/Th1 activation cytokines secretion. Cytokines evaluated were IFN-γ, IL-2, granzyme B, and TNF-α. (D) Quantification of flow cytometric analysis showing CD4<sup>+</sup> CAR T cell intracellular production of Tc1/Th1 activation cytokines when cultured with U937-CD33<sup>high</sup> tumor (n=4; \*\*\*\*p<0.0001, \*p<0.05 by two-way ANOVA). Data are a mean±SEM of four biological replicates conducted in three independent experiments. Cytokines evaluated were IFN-γ, IL-2, granzyme B, and TNF-α. (E) Quantification of flow cytometric analysis showing CD8<sup>+</sup> CAR T cell intracellular production of Tc1/Th1 activation cytokines when cultured with U937-CD33<sup>high</sup> tumor (n=4; \*\*\*p<0.001; \*\*p<0.01; \*p<0.05 by two-way ANOVA). Data are a mean±SEM of four biological replicates conducted in three independent experiments. Cytokines evaluated were IFN-γ, IL-2, granzyme B, and TNF-α. (F) Quantification of flow cytometric analysis demonstrating CAR T cell activation status 7 days post-antigen stimulation with U937-CD33<sup>high</sup> tumor (n=4; \*\*\*\*p<0.0001 by two-way ANOVA). Data are a mean±SEM of four biological replicates conducted in three independent experiments. (G) Qualitative representation of flow cytometric analysis comparing CAR T cell activation profiles. Data are pooled from four biological replicates conducted in three independent experiments.

H195HLh28Z (figure 3B). Furthermore, 3P14HLh28Z had fewer non-secreting CD4<sup>+</sup> cells and more CD4<sup>+</sup> and CD8<sup>+</sup> cells secreting at least two factors as compared with H195HLh28Z. Conversely, 4B2AHLh28Z showed a secretion pattern in between 3P14HLh28Z and H195HLh28Z (figure 3C–E). Given our prior observation of CAR T cell

proliferation at 7 days after U937-CD33<sup>high</sup> encounter (figure 2E), we further characterized these CAR T cells at this timepoint using multiparametric flow cytometry. We observed an increased number of 3P14HLh28Z cells showing an immunophenotype consistent with activation, based on CD69 and HLA-DR (DR) positivity (figure 3F,G).



Collectively, these data suggest that 3P14HLh28Z cells display a polyfunctional soluble factor secreting profile on antigen encounter and demonstrate high levels of activation after antigen encounter.

### CAR T cells targeting CD33-IgC are effective in xenograft models of AML

CD33-directed CAR T cells must demonstrate efficacy at low cell numbers and in the setting of low-antigen-density AML. To determine whether 3P14HLh28Z and 4B2AHLh28Z could control disease in these settings, we inoculated NCG mice with U937-CD33<sup>high</sup> and treated with varying doses of CAR T cells ( $5 \times 10^5$ ,  $2.5 \times 10^5$ ,  $1 \times 10^5$ , and  $5 \times 10^4$ ) 3 days later using a “CAR stress test” model,<sup>26</sup> tracking bioluminescence (BLI) and survival (figure 4A). CD33-IgC-directed CAR T cells demonstrated superior tumor control and improved survival in a dose-dependent manner as compared with H195HLh28Z, while 3P14HLh28Z demonstrated rapid tumor control and prolonged tumor-free states, leading to improved survival at  $2.5 \times 10^5$  and  $5 \times 10^5$  CAR T cell dose levels (figure 4B–D, online supplemental figure 5A–C). At higher doses of CAR T cells ( $2.5 \times 10^6$  and  $1 \times 10^6$ ), H195HLh28Z also controlled tumor and improved survival in NCG mice inoculated with U937-CD33<sup>high</sup> in a dose-dependent manner (online supplemental figure 5D–F). To confirm our findings in another previously published CD33<sup>high</sup> model,<sup>19</sup> we inoculated NCG mice with MOLM14-CD33<sup>high</sup> and treated with  $1 \times 10^6$  CAR T cells 3 days later (online supplemental figure 5G). Results again demonstrated superior tumor control and improved survival of CD33-IgC-directed CAR T cells as compared with H195HLh28Z (online supplemental figure 5H–J).

We subsequently assessed the capacity of these CAR T cells to control tumor growth in the setting of low-antigen-density tumor, using NCG mice engrafted with OCiAML3-CD33<sup>low</sup> (figure 4E). In this setting, 3P14HLh28Z again demonstrated superior tumor control and improved survival as compared with 4B2AHLh28Z, which in turn showed improved survival over H195HLh28Z (figure 4F–H).

Collectively, these data suggest that 3P14HLh28Z CAR T cells have enhanced functionality in both high-antigen-density and low-antigen-density xenograft models, allowing for long-term survival.

### CAR T cells targeting CD33-IgC are effective in a clinically relevant AML PDX model

To demonstrate translational relevance, we established an in vivo model using peripheral blasts from a patient with R/R CD33<sup>+</sup> AML (AML60B; figure 5A,B, online supplemental table 3). AML60B can engraft without conditioning irradiation, allowing for increased tumor burden over time and delayed CAR T cell treatment. Ten days after NCG mice were inoculated, they were randomized and treated with allogeneic H195h28Z, 3P14HLh28Z, or 4B2AHLh28Z CAR T cells (figure 5C). Compared with H195HLh28Z, 3P14HLh28Z and 4B2AHLh28Z conferred

superior tumor control as evaluated on day 28 bone marrow aspiration (figure 5D), with only 3P14HLh28Z-treated mice achieving long-term survival in half of the cohort (figure 5E).

Taken together, these data demonstrate that 3P14HLh28Z provides superior tumor control, leading to long-term survival in vivo in the setting of a clinically relevant tumor model established from R/R primary AML.

## DISCUSSION

Despite the introduction of novel agents to the AML therapeutic armamentarium, this myeloid malignancy continues to have a poor prognosis; there is a critical need for potent interventions such as adoptive T cell therapy. CAR T cells have revolutionized the treatment of B-cell malignancies but have yet to show efficacy in myeloid disease.

Recently, Tambaro *et al* described a phase I trial (NCT03126864) using autologous CD33-directed 4-1BB/CD3Z CAR T cells for the treatment of adult patients with R/R AML.<sup>9</sup> The CAR T cell product was successfully manufactured and administered to only 3 out of 10 enrolled patients, in part due to lymphopenia and inadequate numbers of starting T cells obtained at the apheresis step. None of these three treated patients had observable anti-leukemia response at the first dose level. This study showed that AML-directed CAR T cells must be capable of robust proliferation and killing at low effector-to-tumor ratios, as many patients with R/R AML have lymphopenia and high disease burden of circulating peripheral blasts. Qin *et al* recently described an extensive preclinical screen of CD33 IgV-directed CAR T cells derived from lintuzumab (H195) and gemtuzumab, integrating either CD28/CD3Z or 4-1BB/CD3Z costimulatory domains.<sup>19</sup> This study reported the lintuzumab (H195)-CD28/CD3Z platform as the best-in-class CAR for the treatment of AML. A multicenter phase I/II clinical trial (NCT03971799) is currently underway using the lintuzumab-CD28/CD3Z platform to generate autologous CAR T cells (CD33CART) in children, adolescents, and young adults with R/R AML.<sup>20</sup> Despite wide inter-patient heterogeneity of apheresis products, centralized manufacturing of CD33CART was successful in 23 out of 24 patients.<sup>27</sup> Complete remission (CR) was only seen at dose level 4 ( $1 \times 10^7$ /kg) and achieved in two out of six subjects treated. We hypothesize that the efficacy of CD33-directed CAR T cells could be improved by targeting the membrane-proximal IgC domain of CD33, allowing for more robust T cell functionality and improved tumor control in patients.

In this study, we demonstrated that the potency of CD33 CAR T cells can be markedly increased by using scFvs that target CD33-IgC with high affinity. Interestingly, raising human binders to membrane-proximal epitopes was dependent on IgC immunization, as full-length CD33 immunization always led to the generation of IgV-specific antibodies, suggesting that IgV is an immunodominant

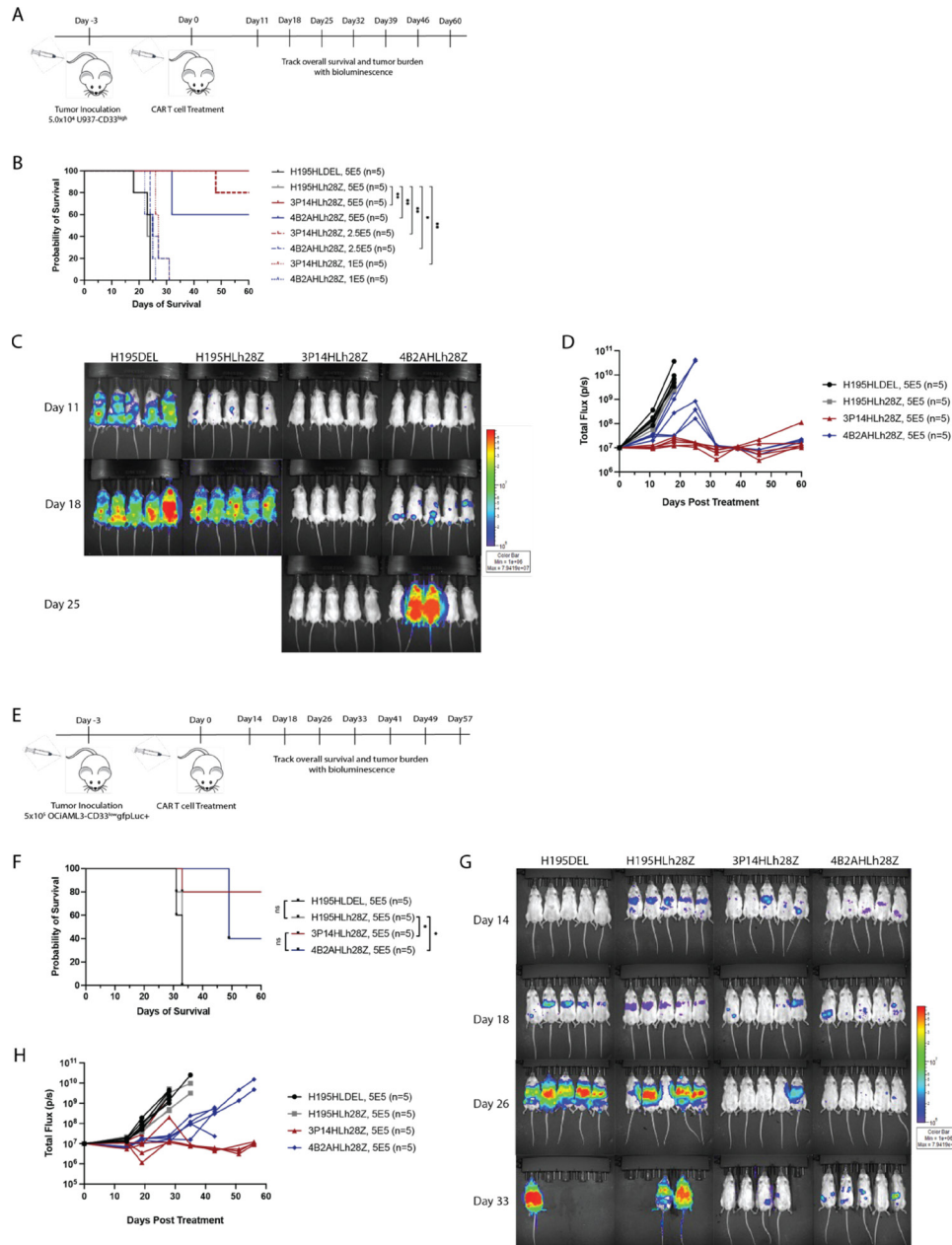


**Figure 4** Membrane-proximal CD33-targeting chimeric antigen receptor (CAR) T cells provide enhanced survival in xenograft mouse model. (A) Schematic diagram of in vivo experimental setup. NCG mice were inoculated with U937-CD33<sup>high</sup> tumor and subsequently treated with CAR T cells. (B) Survival of NCG mice bearing U937-CD33<sup>high</sup> tumors and treated with titrated doses of CAR T cells (n=5; \*\*p<0.01, \*p<0.05). P values for survival determined by log-rank Mantel-Cox test, with 95% CI. (C) Tumor regression of NCG mice inoculated with U937-CD33<sup>high</sup> tumor and subsequently treated with 5.0×10<sup>5</sup> of CAR T cells. (D) Bioluminescence over time of U937-CD33<sup>high</sup> in tumor-bearing NCG mice treated with 5.0×10<sup>5</sup> CAR T cells. (E) Schematic diagram of in vivo experimental setup. NCG mice were inoculated with OCiAML3-CD33<sup>low</sup> tumor and subsequently treated with CAR T cells. (F) Survival of NCG mice inoculated with OCiAML3-CD33<sup>low</sup> tumors and treated with 5.0×10<sup>5</sup> CAR T cells (n=5; \*p<0.05). P values for survival determined by log-rank Mantel-Cox test, with 95% CI. (G) Tumor regression of NCG mice bearing OCiAML3-CD33<sup>low</sup> tumors and treated with 5.0×10<sup>5</sup> CAR T cells. (H) Bioluminescence over time of OCiAML3-CD33<sup>low</sup> in tumor-bearing NCG mice treated with 5.0×10<sup>5</sup> CAR T cells.

epitope in rodents. Importantly, the increased efficacy of high-affinity, membrane-proximal binding CAR T cells depended on their increased capacity for activation and polyfunctionality on antigen encounter, which improved their functionality against tumors with low CD33 antigen density and clinically relevant AML PDXs. H195HL28z proved unsuccessful in effectively controlling this very

aggressive PDX tumor model; we think it is unlikely that AML60B PDX carries the rs12459419 genotype because the CD33 expression level was high (figure 5A). These data suggest that selecting scFvs derived from antibodies targeting membrane-proximal CD33 epitopes with high affinity via domain-specific immunization significantly enhances CAR T cells' efficacy against a CD33-expressing

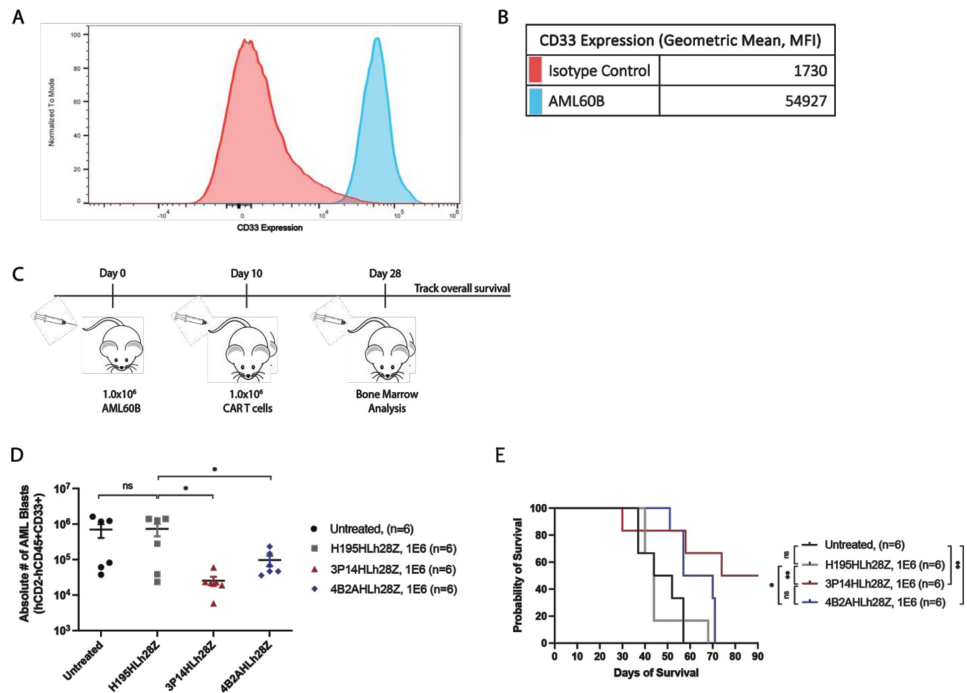


**Figure 5** Membrane-proximal CD33-targeting chimeric antigen receptor (CAR) T cells decrease tumor burden in patient-derived acute myeloid leukemia (AML) xenograft model. (A) Flow cytometry histograms of CD33 expression on AML60B patient sample detected with isotype control or fluorescently labeled CD33-specific antibody. (B) Quantitative geometric mean fluorescence intensity (MFI) of CD33 expression on AML60B patient sample detected with either isotype control or fluorescently labeled CD33-specific antibody. (C) Schematic diagram of experimental setup of a patient-derived xenograft model. NCG mice were inoculated with patient-derived AML blasts and treated with allogeneic CAR T cells. Bone marrow aspirates were analyzed 28 days post tumor inoculation. (D) Quantification of flow cytometric analysis demonstrating decreased tumor burden in mice treated with membrane-proximal CD33-targeting CAR T cells (n=6; \*p<0.05 by unpaired t-test). (E) Survival of NCG mice-bearing AML60B patient-derived tumor and treated with membrane-distal or membrane-proximal CAR T cells (n=6; \*\*p<0.01; \*p<0.05). P values for survival determined by log-rank Mantel-Cox test, with 95% CI.

target compared with scFvs derived from low-affinity membrane proximal and high-affinity membrane distal binders.

Further investigation into the mechanism of improved efficacy of the high-affinity membrane-proximal CAR T cells is warranted. For example, testing a variety of hinge lengths is a key step in further optimization of this CAR construct, especially as preparation for clinical translation of this CAR product. Additionally, further investigation into mechanisms of tumor escape after initial control in vivo is also warranted. For the mice who had initial tumor control and then relapsed, although it is possible that CD33 downregulation was a mediator of disease escape, in this “CAR stress test” model our dose of CAR T cells was suboptimal and could explain why disease relapse occurred. However, mechanisms of escape are of great interest in translating this product to clinic, and efforts to establish PDX models with CD33-low patient tumors are currently underway.

Although the clinical relevance of the CD33 rs12459419 C>T SNP, which is associated with decreased/absent CD33 surface expression,<sup>13 14</sup> remains controversial, we see robustly in all three of our CD33-expressing AML models (CC, CT, and TT) that the membrane-proximal binders outperform the membrane-distal binders, and so it is unlikely that our membrane-proximal binders’

efficacy is due to isoform variability alone. Furthermore, there is conflicting data on the relevance of the SNP in clinical outcomes, and it remains controversial whether the TT polymorphism results in an isoform that lacks the IgV domain completely<sup>15</sup> or rather decreases the amount of wild-type CD33.<sup>28</sup> However, based on our data, it seems that the TT genotype (OCIAML3) still has some level of wild-type CD33, which is why it is sensitive to killing by H195HL28z.

Our findings align with others demonstrating the advantage of targeting membrane-proximal epitopes through CAR T cells and T-cell-dependent bispecifics. Godwin *et al* demonstrated that, compared with targeting full-length CD33, ectopic expression of C33-IgV in a membrane-proximal position led to improved IgV-directed CAR T cell function.<sup>21</sup> However, the role of scFv affinity in enhancing CAR T cell efficacy is less clear, as both low-affinity and high-affinity CAR T cells have relatively increased efficacy.<sup>29 30</sup> Although both the high-affinity and low-affinity membrane-proximal binders had similar in vitro cytotoxicity profiles, significant differences in 3P14 versus 4B2A proliferation were likely due to affinity of the 3p14 scFv for CD33, and 3P14 enacts a more potent stimulatory signal. Killing and proliferation (although both T cell effector function readouts) are not necessarily always concordant, and this potentially explains why we see such

robust differences between killing and proliferation. Our results suggest that whether affinity enhances CAR T cell efficacy may depend on the nature of the target as well as the location of the epitope, with more potent activity of high-affinity scFvs to membrane-proximal epitopes on immunoglobulin-like targets.

HSC ablation is an important consideration when targeting CD33, which is also expressed on these non-malignant cells. Our high-affinity, membrane-proximal CAR T cells completely ablated umbilical cord blood-derived colony formation, while our low-affinity, membrane-proximal and lintuzumab-derived CAR T cells did not. H195HLh28z did not eradicate CFUs while GO did because H195HLh28z is likely not killing low antigen density HSCs.<sup>31–32</sup> Furthermore, although GO was used as a positive control in this experiment, it is difficult to titrate/compare antibody-drug conjugates to CARs. Therefore, it is very likely that the concentration of GO used was able to eradicate more CFUs. Additionally, there is a strong possibility of bystander killing with antibody-drug conjugates, which might further confound these results.<sup>33</sup> Importantly, only our high-affinity, membrane-proximal CAR T cells provided complete disease control in both low antigen density and clinically relevant patient-derived xenograft models. Of great clinical relevance, this suggests that there might be no feasible therapeutic window for targeting CD33, because reduced antigen recognition by CAR T cells while sparing HSCs would allow for escape of low-antigen-density malignant subpopulations that have been implicated as critical mediators of clinical failure of CAR T cell therapy. Strategies to address the myeloablative capacity of our high-affinity, membrane-proximal CAR T cells include: (1) use of the CD28/CD3Z costimulatory domain, which allows for rapid tumor clearance with limited T cell persistence,<sup>34</sup> (2) integration of an elimination switch to allow for CAR T cell elimination,<sup>35</sup> (3) rescue allogeneic stem cell transplantation, or (4) reconstitution of hematopoiesis with HSCs in which CD33 has been deleted. Future research will address the potential of these interventions to minimize the hematopoietic toxicity of our novel CAR T cell platform.

In summary, our results demonstrate that the efficacy of CD33-targeted CAR T cells can be markedly improved through membrane-proximal targeting with a high-affinity scFv raised through epitope-specific immunization. These CAR T cells have improved activation and polyfunctionality as well as enhanced capacity to eliminate disease with low antigen density or clinically relevant PDX models.

**Acknowledgements** We thank the MSK Antitumor Assessment Core Facility for excellent technical assistance. Editorial support was provided by Hannah Rice, BA, ELS, Katharine Olla, MA, and Joseph Olechnowicz, MA at Memorial Sloan Kettering Cancer Center.

**Contributors** RF, AGK, and ICL conceived ideas for study design. RF, S Shahid, AGK, SM, S Souness, ERB, JSU, KT, WC, SY, A Dunbar, YP, DM, KKH, ICL, RJB, and A Daniyan designed and performed experiments, and analyzed data. RF, S Shahid, RJB, and A Daniyan wrote the manuscript. RL and JJB provided advice and support.

RJB and A Daniyan were the principal investigators of the study and conceived the idea, designed, analyzed, and supervised the study and wrote the manuscript. RJB is responsible for the overall content as the guarantor.

**Funding** This work was supported in part by Memorial Sloan Kettering Cancer Center Support Grant/Core Grant (P30 CA008748), the Geoffrey Beene Cancer Research Center (#18181), MSK Tri-Institutional Therapeutics Discovery Institute (TDI), NIH NCI (19348[NIH 1P50CA254838 01(MSK SPORE in Leukemia)]), and NIH NCI P01 CA108671 11 as well as funding from the Annual Terry Fox Run for Cancer Research organized by the Canada Club of New York (Kate's Team), Stacey and Robert Morse, Comedy vs Cancer, and Edward P. Evans Foundation Award Fund (#19291). RF, SM, WC, RJB, and AFD are supported by Geoffrey Beene Cancer Research Center. AFD is supported by K12 CA184746. The authors gratefully acknowledge the support to the project generously provided by the Tri-Institutional Therapeutics Discovery Institute (TDI), a 501(c)(3) organization. TDI receives financial support from Takeda Pharmaceutical Company, TDI's parent institutes (Memorial Sloan Kettering Cancer Center, The Rockefeller University and Weill Cornell Medicine), and from Lewis Sanders and other philanthropic sources.

**Competing interests** AGK, ICL, RJB, and A Daniyan have filed provisional patent applications covering applications of membrane-proximal CD33 binders for cellular therapy. A Dunbar, YP, and RL are supported by National Cancer Institute P01 CA108671 11 (RL). DM and KKH are supported by an MSK Geoffrey Beene Cancer Research Award. RL is on the supervisory board of Qiagen and is a scientific advisor to Imago, Mission Bio, Zentalis, Ajax, Auron, Prelude, C4 Therapeutics and Isoplexis. He receives research support from and consulted for Celgene and Roche and has consulted for Incyte, Janssen, Astellas, Morphosys and Novartis, and has received honoraria from AstraZeneca, Roche, Lilly and Amgen for invited lectures and from Gilead for grant reviews. JJB has consulted for Avrobio, Sobi, BlueRock, Sanofi, Omeros, Advanced Clinical, MERCK, Bluebird Bio and is on the Data Safety Monitoring Board/Advisory Board for Advanced Clinical. RJB has licensed intellectual property to and collects royalties from BMS, Caribou, and Sanofi. RJB received research funding from BMS. RJB is a consultant to BMS, Atara Biotherapeutics Inc, Cargo Tx, Triumvira and was a consultant for Colmmune but ended in the past 3 months and Gracell Biotechnologies Inc but ended employment in the past 24 months. RJB is a member of the scientific advisory board for Triumvira, Cargo Tx and was a member of the scientific advisory board for Colmmune, but that ended in the past 3 months.

**Patient consent for publication** Not applicable.

**Ethics approval** Not applicable.

**Provenance and peer review** Not commissioned; externally peer reviewed.

**Data availability statement** All data relevant to the study are included in the article or uploaded as supplementary information.

**Supplemental material** This content has been supplied by the author(s). It has not been vetted by BMJ Publishing Group Limited (BMJ) and may not have been peer-reviewed. Any opinions or recommendations discussed are solely those of the author(s) and are not endorsed by BMJ. BMJ disclaims all liability and responsibility arising from any reliance placed on the content. Where the content includes any translated material, BMJ does not warrant the accuracy and reliability of the translations (including but not limited to local regulations, clinical guidelines, terminology, drug names and drug dosages), and is not responsible for any error and/or omissions arising from translation and adaptation or otherwise.

**Open access** This is an open access article distributed in accordance with the Creative Commons Attribution Non Commercial (CC BY-NC 4.0) license, which permits others to distribute, remix, adapt, build upon this work non-commercially, and license their derivative works on different terms, provided the original work is properly cited, appropriate credit is given, any changes made indicated, and the use is non-commercial. See <http://creativecommons.org/licenses/by-nc/4.0/>.

#### ORCID iDs

Sanam Shahid <http://orcid.org/0000-0003-4281-4910>

Anthony F Daniyan <http://orcid.org/0009-0002-2742-2281>

#### REFERENCES

- 1 Ganzel C, Sun Z, Cripe LD, *et al*. Very poor long-term survival in past and more recent studies for relapsed AML patients: the ECOG-ACRIN experience. *Am J Hematol* 2018;93:1074–81.
- 2 Vitale C, Strati P. CAR T-cell therapy for B-cell non-Hodgkin lymphoma and chronic lymphocytic leukemia: clinical trials and real-world experiences. *Front Oncol* 2020;10:849.

- 3 Martino M, Alati C, Canale FA, *et al.* A review of clinical outcomes of CAR T-cell therapies for B-acute lymphoblastic leukemia. *Int J Mol Sci* 2021;22:2150.
- 4 Majzner RG, Rietberg SP, Sotillo E, *et al.* Tuning the antigen density requirement for CAR T-cell activity. *Cancer Discov* 2020;10:702–23.
- 5 Spiegel JY, Patel S, Muffly L, *et al.* CAR T cells with dual targeting of CD19 and CD22 in adult patients with recurrent or refractory B cell malignancies: a phase 1 trial. *Nat Med* 2021;27:1419–31.
- 6 Rossi J, Paczkowski P, Shen Y-W, *et al.* Preinfusion polyfunctional anti-CD19 Chimeric antigen receptor T cells are associated with clinical outcomes in NHL. *Blood* 2018;132:804–14.
- 7 Davis JL, Theoret MR, Zheng Z, *et al.* Development of human anti-murine T-cell receptor antibodies in both responding and nonresponding patients enrolled in TCR gene therapy trials. *Clin Cancer Res* 2010;16:5852–61.
- 8 Maus MV, Haas AR, Beatty GL, *et al.* T cells expressing chimeric antigen receptors can cause anaphylaxis in humans. *Cancer Immunol Res* 2013;1:26–31.
- 9 Tambaro FP, Singh H, Jones E, *et al.* Autologous CD33-CAR-T cells for treatment of relapsed/refractory acute myelogenous leukemia. *Leukemia* 2021;35:3282–6.
- 10 Perna F, Berman SH, Soni RK, *et al.* Integrating proteomics and transcriptomics for systematic combinatorial chimeric antigen receptor therapy of AML. *Cancer Cell* 2017;32:506–19.
- 11 Borot F, Wang H, Ma Y, *et al.* Gene-edited stem cells enable CD33-directed immune therapy for myeloid malignancies. *Proc Natl Acad Sci U S A* 2019;116:11978–87.
- 12 Kim MY, Yu K-R, Kenderian SS, *et al.* Genetic inactivation of CD33 in hematopoietic stem cells to enable CAR T cell immunotherapy for acute myeloid leukemia. *Cell* 2018;173:1439–53.
- 13 Mortland L, Alonzo TA, Walter RB, *et al.* Clinical significance of Cd33 Nonsynonymous single-nucleotide Polymorphisms in pediatric patients with acute myeloid leukemia treated with Gemtuzumab-Ozogamicin-containing chemotherapy. *Clin Cancer Res* 2013;19:1620–7.
- 14 Laszlo GS, Beddoe ME, Godwin CD, *et al.* Relationship between CD33 expression, splicing polymorphism, and in vitro cytotoxicity of gemtuzumab ozogamicin and the CD33/CD3 Bite(R). *Haematologica* 2019;104:e59–62.
- 15 Lamba JK, Chauhan L, Shin M, *et al.* CD33 splicing polymorphism determines gemtuzumab ozogamicin response in de novo acute myeloid leukemia: report from randomized phase III children's oncology group trial AAML0531. *J Clin Oncol* 2017;35:2674–82.
- 16 Gale RE, Popa T, Wright M, *et al.* No evidence that CD33 splicing SNP impacts the response to GO in younger adults with AML treated on UK MRC/NCRI trials. *Blood* 2018;131:468–71.
- 17 Kenderian SS, Ruella M, Shestova O, *et al.* CD33-specific chimeric antigen receptor T cells exhibit potent preclinical activity against human acute myeloid leukemia. *Leukemia* 2015;29:1637–47.
- 18 O'Hear C, Heiber JF, Schubert I, *et al.* Anti-CD33 Chimeric antigen receptor targeting of acute myeloid leukemia. *Haematologica* 2015;100:336–44.
- 19 Qin H, Yang L, Chukinas JA, *et al.* Systematic preclinical evaluation of CD33-directed chimeric antigen receptor T cell immunotherapy for acute myeloid leukemia defines optimized construct design. *J Immunother Cancer* 2021;9:e003149.
- 20 Shah NN, Tasian SK, Kohler ME, *et al.* CD33 CAR T-cells (CD33CART) for children and young adults with relapsed/refractory AML: dose-escalation results from a phase I/II multicenter trial. *Blood* 2023;142:771.
- 21 Godwin CD, Laszlo GS, Fiorenza S, *et al.* Targeting the membrane-proximal C2-set domain of CD33 for improved CD33-directed Immunotherapy. *Leukemia* 2021;35:2496–507.
- 22 Haso W, Lee DW, Shah NN, *et al.* Anti-CD22-Chimeric antigen receptors targeting B-cell precursor acute lymphoblastic leukemia. *Blood* 2013;121:1165–74.
- 23 Zhang Z, Jiang D, Yang H, *et al.* Modified CAR T cells targeting membrane-proximal EPITOPE of mesothelin enhances the antitumor function against large solid tumor. *Cell Death Dis* 2019;10:476.
- 24 Li J, Stagg NJ, Johnston J, *et al.* Membrane-proximal EPITOPE facilitates efficient T cell synapse formation by anti-FcRH5/CD3 and is a requirement for myeloma cell killing. *Cancer Cell* 2017;31:383–95.
- 25 Locke FL, Rossi JM, Neelapu SS, *et al.* Tumor burden, inflammation, and product attributes determine outcomes of axicabtagene ciloleucel in large B-cell lymphoma. *Blood Adv* 2020;4:4898–911.
- 26 Eyquem J, Mansilla-Soto J, Giavridis T, *et al.* Targeting a CAR to the TRAC locus with CRISPR/Cas9 enhances tumour rejection. *Nature* 2017;543:113–7.
- 27 Bowser B, Yang X, Roach J, *et al.* Success of centralized manufacturing of CD33 CAR T-cells (Cd33Cart) for children and young adults with relapsed/refractory AML. *Transplantation and Cellular Therapy* 2024;30:S153–4.
- 28 Oya S, Ozawa H, Nakamura T, *et al.* CD33 rs12459419 SNP regulated the total CD33 expression level. *Blood* 2022;140:11784–5.
- 29 Abbott RC, Verdon DJ, Gracey FM, *et al.* Novel high-affinity Egrfviii-specific chimeric antigen receptor T cells effectively eliminate human glioblastoma. *Clin Transl Immunology* 2021;10:e1283.
- 30 Ghorashian S, Kramer AM, Onuoha S, *et al.* Enhanced CAR T cell expansion and prolonged persistence in pediatric patients with ALL treated with a low-affinity Cd19 CAR. *Nat Med* 2019;25:1408–14.
- 31 Hauswirth AW, Florian S, Printz D, *et al.* Expression of the target receptor CD33 in CD34+/CD38–/CD123+ AML stem cells. *Eur J Clin Invest* 2007;37:73–82.
- 32 Arndt C, von Bonin M, Cartellieri M, *et al.* Redirection of T cells with a first fully humanized bispecific CD33–CD3 antibody efficiently eliminates AML blasts without harming hematopoietic stem cells. *Leukemia* 2013;27:964–7.
- 33 Staudacher AH, Brown MP. Antibody drug conjugates and bystander killing: is antigen-dependent internalisation required *Br J Cancer* 2017;117:1736–42.
- 34 Long AH, Haso WM, Shern JF, *et al.* 4-1Bb Costimulation ameliorates T cell exhaustion induced by tonic signaling of chimeric antigen receptors. *Nat Med* 2015;21:581–90.
- 35 Moghanloo E, Mollanoori H, Talebi M, *et al.* Remote controlling of CAR-T cells and toxicity management: molecular switches and next generation cars. *Transl Oncol* 2021;14:101070.